A&A 390, 187–198 (2002)
DOI: 10.1051/0004-6361:20020687

Astronomy & Astrophysics

First Stars
II. Elemental abundances in the extremely metal-poor star CS 22949–037⋆

A diagnostic of early massive supernovae

E. Depagne[1], V. Hill[1], M. Spite[1], F. Spite[1], B. Plez[2], T. C. Beers[3], B. Barbuy[4], R. Cayrel[1], J. Andersen[5], P. Bonifacio[6], P. François[1], B. Nordström[7,5], and F. Primas[8]

[1] Observatoire de Paris-Meudon, GEPI, 92195 Meudon Cedex, France
e-mail: Vanessa.Hill@obspm.fr, Roger.Cayrel@obspm.fr
e-mail: Monique.Spite@obspm.fr, Francois.Spite@obspm.fr, Patrick.Francois@obspm.fr
[2] GRAAL, Université de Montpellier II, 34095 Montpellier Cedex 05, France
e-mail: Bertrand.Plez@graal.univ-montp2.fr
[3] Department of Physics & Astronomy, Michigan State University, East Lansing, MI 48824, USA
e-mail: beers@pa.msu.edu
[4] IAG, Universidade de São Paulo, Departamento de Astronomia, CP 3386, 01060-970 São Paulo, Brazil
e-mail: barbuy@astro.iag.usp.br
[5] Astronomical Observatory, NBIfAFG, Juliane Maries Vej 30, 2100 Copenhagen, Denmark
e-mail: ja@astro.ku.dk
[6] Istituto Nazionale di Astrofisica – Osservatorio Astronomico di Trieste, Via G.B. Tiepolo 11, 34131 Trieste, Italy
e-mail: bonifaci@ts.astro.it
[7] Lund Observatory, Box 43, 221 00 Lund, Sweden
e-mail: birgitta@astro.lu.se
[8] European Southern Observatory (ESO), Karl-Schwarschild-Str. 2, 85749 Garching b. München, Germany
e-mail: fprimas@eso.org

Received 14 February 2002 / Accepted 3 May 2002

Abstract. CS 22949–037 is one of the most metal-poor giants known ([Fe/H] ≈ −4.0), and it exhibits large overabundances of carbon and nitrogen (Norris et al.). Using VLT-UVES spectra of unprecedented quality, regarding resolution and S/N ratio, covering a wide wavelength range (from λ = 350 to 900 nm), we have determined abundances for 21 elements in this star over a wide range of atomic mass. The major new discovery is an exceptionally large oxygen enhancement, [O/Fe] = 1.97 ± 0.1, as measured from the [O I] line at 630.0 nm. We find an enhancement of [N/Fe] of 2.56 ± 0.2, and a milder one of [C/Fe] = 1.17 ± 0.1, similar to those already reported in the literature. This implies $Z_\star = 0.01\ Z_\odot$. We also find carbon isotopic ratios $^{12}C/^{13}C = 4 \pm 2.0$ and $^{13}C/^{14}N = 0.03^{+0.035}_{-0.015}$, close to the equilibrium value of the CN cycle. Lithium is not detected. Na is strongly enhanced ([Na/Fe] = +2.1 ± 0.2), while S and K are not detected. The silicon-burning elements Cr and Mn are underabundant, while Co and Zn are overabundant ([Zn/Fe] = +0.7). Zn is measured for the first time in such an extremely metal-poor star. The abundances of the neutron-capture elements Sr, Y, and Ba are strongly decreasing with the atomic number of the element: [Sr/Fe] ≈ +0.3, [Y/Fe] ≈ −0.1, and [Ba/Fe] ≈ −0.6. Among possible progenitors of CS 22949–037, we discuss the pair-instability supernovae. Such very massive objects indeed produce large amounts of oxygen, and have been found to be possible sources of primary nitrogen. However, the predicted odd/even effect is too large, and the predicted Zn abundance much too low. Other scenarios are also discussed. In particular, the yields of a recent model (Z35Z) from Heger and Woosley are shown to be in fair agreement with the observations. The only discrepant prediction is the very low abundance of nitrogen, possibly curable by taking into account other effects such as rotationally induced mixing. Alternatively, the absence of lithium in our star, and the values of the isotopic ratios $^{12}C/^{13}C$ and $^{13}C/^{14}N$ close to the equilibrium value of the CN cycle, suggest that the CNO abundances now observed might have been altered by nuclear processing in the star itself. A 30–40 $M_\odot$ supernova, with fallback, seems the most likely progenitor for CS 22949–037.

Key words. stars: fundamental parameters – stars: abundances – stars: individual: BPS CS 22949–037 – Galaxy: evolution

Send offprint requests to: E. Depagne,
e-mail: Eric.Depagne@obspm.fr

⋆ Based on observations made with the ESO Very Large Telescope at Paranal Observatory, Chile (programme ID 165.N-0276(A)).

1. Introduction

The element abundances in the most metal-poor stars provide the fossil record of the earliest nucleosynthesis events in the Galaxy, and hence allow the study of Galactic chemical evolution in its earliest phases. Moreover, such data can have *cosmological* implications: radioactive age determinations (Cowan et al. 1999; Cayrel et al. 2001) provide an independent lower limit to the age of the Universe, and the lithium abundance in metal-poor dwarfs is an important constraint on the baryonic content of the Universe (Spite & Spite 1982). The dispersion of the observed abundance ratios for a number of elements in extremely metal-poor (XMP) stars is very large, reflecting the yields of progenitors of different masses, and indicating that each star has been formed from material processed by a small number of supernova events – perhaps only one. Thus, the detailed chemical composition of XMP stars provides constraints on the properties of the very first supernovae (and hypernovae?) events in our Galaxy. Accordingly, the past decade has seen a rapidly growing interest in the detailed chemical composition of XMP stars.

BPS CS 22947–037, discovered in the HK survey of Beers et al. (1992, 1999), is one of the lowest metallicity halo giants known ([Fe/H] ≈ -4.0). Several studies (McWilliam et al. 1995; Norris et al. 2001) have shown that this star exhibits a highly unusual chemical composition, characterised by exceptionally large enhancements of the lightest α elements: Norris et al. (2001) found [Mg/Fe] = +1.2, [Si/Fe] = +1.0, [Ca/Fe] = +0.45, and even more dramatic values for carbon and especially nitrogen: [C/Fe] = +1.1 and [N/Fe] = +2.7. In contrast, the abundance of the neutron-capture elements was found to be rather low: [Ba/Fe] = −0.77.

These abundance ratios cannot be explained by classical mixing processes between the surface of the star and deep CNO-processed layers, or by the enrichment of primordial material by the ejecta of standard supernovae. Canonical supernova and Galactic Chemical Evolution (GCE) models (Timmes et al. 1995) predict that [C/Fe] should be solar, and [N/Fe] subsolar (since N is produced as a secondary element). Norris et al. (2001) discuss a variety of scenarios to explain this abundance pattern, and finally suggest that the material from which the star was formed was enriched by the ejecta from a massive zero-heavy-element hypernova (>200 $M_{\odot}$), which might be able to produce large amounts of primary nitrogen via proton capture on dredged-up carbon.

However, no previous analysis has yielded a measurement of the abundance of oxygen, an extremely important element, both for the precise determination of the nitrogen abundance and as a key diagnostic of alternative progenitor scenarios. We have therefore observed CS 22949–037 in the framework of a large, systematic programme on XMP stars with the ESO VLT and its UVES spectrograph. The extended wavelength coverage (including the red region), superior resolution, and S/N of our spectra enable us to determine abundances for a large sample of elements with unprecedented accuracy, accounting for the abundance anomalies of the star in a self-consistent manner, especially in the opacity computation.

This paper presents these new results and discusses their astrophysical implications. In Sect. 2 the observations are sumarized. Section 3 presents a description of the model atmosphere calculations, and the methods used in the elemental abundance analyses. In Sect. 4 the observed abundance pattern for CS 22949–037 is compared with predictions of recent supernova and hypernova models.

2. Spectroscopic observations

The observations were performed in August 2000 and September 2001 at the VLT-UT2 with the high-resolution spectrograph UVES (Dekker et al. 2000). The spectrograph settings (dichroic mode, central wavelength 396 nm in the blue arm, and 573 or 850 nm in the red arm) provide almost complete spectral coverage from ∼330 to 1000 nm. A 1″ entrance slit yielded a resolving power of $R \sim 45\,000$.

For CS 22949–037 ($V = 14.36$) we accumulated a total integration time of 7 hours in the blue, 4 hours in the setting centered at 573 nm, and 3 hours in the setting centered at 850 nm. Table 1 provides the observing log, together with the final S/N obtained at three typical wavelengths, and the barycentric radial velocity of the star at the time of the observation.

The spectra were reduced using the UVES package within MIDAS, which performs bias and inter-order background subtraction (object and flat-field), optimal extraction of the object (above sky, rejecting cosmic ray hits), division by a flat-field frame extracted with the same weighted profile as the object, wavelength calibration and rebinning to a constant wavelength, and step and merging of all overlapping orders. The spectra were then co-added and normalised to unity in the continuum. The mean spectrum from August 2000 has been used for the abundance analysis. The spectrum from September 2001 has a lower S/N ratio, and has been used only to check for radial velocity variations and as a check of the oxygen line profile.

Table 1 gives the barycentric radial velocity for each spectrum of CS 22949–037. The zero-point was derived from the telluric absorption lines (accurate wavelengths of these lines were taken from the GEISA database). The mean value is $V_{\rm r} = -125.64 \pm 0.12$ km s^{-1} (internal error). Note that McWilliam et al. (1995) reported a heliocentric velocity $V_{\rm r} = -126.4 \pm 0.5$ km s^{-1} in 1990, while Norris et al. (2001) obtained $V_{\rm r} = -125.7 \pm 0.2$ km s^{-1} in September 2000. Hence, there is so far no evidence of any significant variation of the radial velocity, and thus no indication that CS 22949–037 might be part of a binary system.

3. Stellar parameters and abundances

3.1. Methods

The abundance analysis was performed with the LTE spectral analysis code "turbospectrum" in conjunction with OSMARCS atmosphere models. The OSMARCS models were originally developed by Gustafsson et al. (1975) and later improved by Plez et al. (1992), Edvardsson et al. (1993), and Asplund et al. (1997). Turbospectrum is described by Alvarez & Plez (1998) and Hill et al. (2002), and has recently been further improved by B. Plez.

Table 1. Log of the UVES observations. S/N refers to the signal-to-noise ratio pixel at 420, 630, and 720 nm in the mean spectrum. There are between 6.7 and 8.3 pixels per resolution element.

date	UT	Setting	Exp. time	V_r km s^{-1}	420 nm	630 nm	720 nm
2000-08-08	04:54	396–573	1 h	−125.68 ± 0.2			
2000-08-08	05:57	396–850	1 h				
2000-08-09	05:04	396–573	1 h	−125.64 ± 0.2			
2000-08-09	04:01	396–850	1 h				
2000-08-11	04:27	396–573	1 h	−125.60 ± 0.2			
2000-08-11	05:36	396–850	1 h				
Global S/N per pixel (2000/08)					110	170	110
Global S/N per resolution element					285	490	320
2001-09-06	05:06	396–573	1 h	−125.62 ± 0.2			
S/N per pixel (2001/09)					40	90	-

The temperature of the star was estimated from the colour indices (Table 2) using the Alonso et al. (1999) calibration for giants. There is good agreement between the temperature deduced from $B-V$, $V-R$ and $V-K$. However, Aoki et al. (2002) have shown that, in metal-deficient carbon-enhanced stars, the temperature determination from a comparison of broad-band colours with temperature scales computed with standard model atmospheres is sometimes problematic, because of the strong absorption bands from carbon-bearing molecules. In the case of CS 22949–037, although carbon and nitrogen are strongly enhanced relative to iron, the molecular bands are in fact never strong because the iron content of the star is so extremely low (ten times below that of stars analysed by Aoki et al. 2000). Neither the red CN system nor the C_2 Swan system are visible, and the blue CH and CN bands remain weak and hardly affect the blanketing in this region (cf. Sect. 3.2.1). Moreover, an independent Balmer-line index analysis yields $T_{\rm eff}$ = 4900 K ±125 K, in excellent agreement with the result from the colour indices and with the value adopted by Norris et al. (2001).

With our final adopted temperature, $T_{\rm eff}$ = 4900 K, the abundance derived from individual Fe I lines is almost independent of excitation potential (Fig. 1), at least for excitation potentials larger than 1.0 eV. Low-excitation lines are more sensitive to non-LTE effects, and the slight overabundance found from the lowest-excitation lines is generally explained by this effect (see also Norris et al. 2001).

The microturbulent velocity was determined by the requirement that the abundances derived from individual Fe I lines be independent of equivalent width. Finally, the surface gravity was determined by demanding that lines of the neutral and first-ionized species of Fe and Ti yield identical abundances of iron and titanium, respectively.

Table 2 compares the resulting atmospheric parameters to those adopted by McWilliam et al. (1995) and Norris et al. (2001).

3.2. Abundance determinations

The measured equivalent widths of all the lines are given in the appendix, together with the adopted atomic transition probabilities and the logarithmic abundance of the element deduced from each line. The error on the equivalent width of the line depends on the S/N ratio of the spectrum and thus on the wavelength of the line (Table 1). Following Cayrel (1988), the error of the equivalent width should be about 1 mÅ in the blue part of the spectrum and less than 0.5 mÅ in the red. Since all the lines are weak, the error on the abundance of the element depends linearly on the error of the equivalent width. In some cases (where complications due to hyper-fine structure, molecular bands, or blends are present) the abundance of the element has been determined by a direct fit of the computed spectrum to the observations.

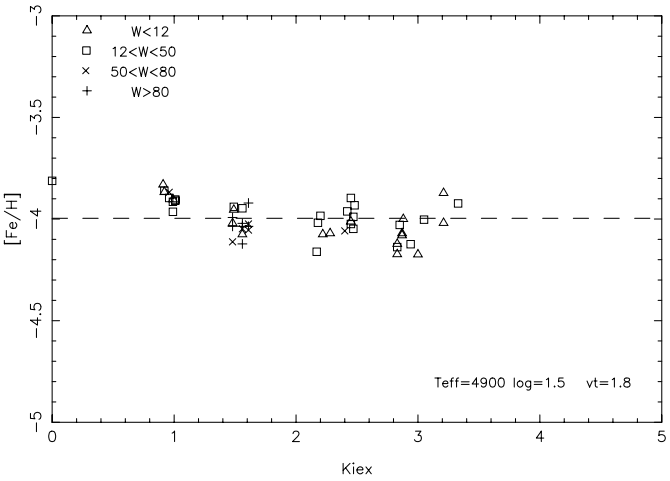

Fig. 1. Iron abundance as a function of excitation potential of the line. Symbols indicate different line strengths (in mÅ).

Table 3 lists the derived [Fe/H] and individual elemental abundance ratios, [X/Fe]. The iron abundance measured here is in good agreement with the results by McWilliam et al. (1995) and Norris et al. (2001): with an iron abundance ten thousand times below that of the Sun, CS 22949–037 is one of the most metal-poor stars known today.

As expected for a giant star, the lithium line is not detected.

Table 2. Colour indices and adopted stellar parameters for CS 22949–037. Temperatures have been computed from the Alonso et al. (1999) relations for $E(B-V) \approx 0.03$ (Burstein & Heiles 1982). The reddening for different colours has been computed following Bessell & Brett (1988).

CS 22949–037 Magnitude or Colour		Ref	Colour corrected for reddening	$T_{\rm eff}$ (Alonso)
V	14.36	1		
$(B-V)$	0.730	1	0.700	4920
$(V-R)_J$	0.715	2	0.695	4910
$(V-K)$	2.298	3	2.215	4880

Adopted parameters for CS 22949–037

$T_{\rm eff}$	$\log g$	[Fe/H]	$v_{\rm t}$	Ref
4810	2.1	−3.5	2.1	1
4900	1.7	−3.8	2.0	4
4900	**1.5**	**−3.9**	**1.8**	**5**

References:
1 Beers et al., in preparation.
2 McWilliam et al. (1995).
3 Point source catalog, 2MASS survey.
4 Norris et al. (2001).
5 Present investigation.

3.2.1. CNO abundances and the $^{12}C/^{13}C$ ratio

The C and N abundances are based on spectrum synthesis of molecular features due to CH and CN. In cool giants, a significant amount of CN and CO molecules are formed and thus, in principle, the C, N, and O abundances cannot be determined independently. However, since CS 22949–037 is relatively warm, little CO is formed, and the abundance of C is not greatly dependent on the O abundance. Nevertheless, we have determined the C, N and O abundances by successive iterations and, in particular, the final iteration has been performed with a model that takes the observed anomalous abundances of these species into account in a self-consistent manner, notably in the opacity calculations.

Carbon and nitrogen

The carbon abundance of CS 22949–037 has been deduced from the $A^2\Delta$–$X^2\Pi$ G band of CH (bandhead at 4323 Å), and the nitrogen abundance from the $B^2\Sigma - X^2\Sigma$ CN violet system (bandhead at 3883 Å). Neither the $A^3\Pi_g - X^3\Pi_u$ C_2 Swan band nor the $A^2\Pi - X^2\Sigma$ red CN band, which are often used for abundance determinations, are visible in this star. Line lists for ^{12}CH, ^{13}CH, $^{12}C^{14}N$, and $^{13}C^{14}N$ were included in the synthesis. The CN line lists were prepared in a similar manner as the TiO line lists of Plez (1998), using data from Cerny et al. (1978), Kotlar et al. (1980), Larsson et al. (1983), Bauschlicher et al. (1988), Ito et al. (1988), Prasad & Bernath (1992), Prasad et al. (1992), and Rehfuss et al. (1992). Programs by Kotlar were used to compute wavenumbers of transitions in the red bands studied by Kotlar et al. (1980). For CH, the LIFBASE program of Luque & Crosley (1999) was used to compute line positions and gf-values. Excitation energies and isotopic shifts were taken from the line list of Jörgensen et al. (1996), as LIFBASE only provides line positions for ^{12}CH. This procedure yielded a good fit of the CH lines, except for a very few lines which were removed from the list. Figure 2 shows the fit of the CN blue system.

Table 3. Individual element abundances. For each element X, Col. 2 gives the mean abundance $\log\epsilon(\mathrm{X}) = \log N_{\rm X}/N_{\rm H} + 12$, Col. 3 the number of lines measured, Col. 4 the standard deviation of the results, and Cols. 5 and 6 [X/H] and [X/Fe], respectively (where $[\mathrm{X/H}] = \log\epsilon(\mathrm{X}) - \log\epsilon(\mathrm{X})_\odot$).

Element	$\log\epsilon(X)$	n	σ	[X/H]	[X/Fe]
Fe I	3.51	64	0.11	−3.99	
Fe II	3.56	6	0.11	−3.94	
C (CH)	5.72		synth	−2.80	+1.17
N (CN)	6.52		synth	−1.40	+2.57
O I	6.84	1	-	−1.99	+1.98
Na I	3.80	2	0.03	−1.88	+2.09
Mg I	5.17	4	0.19	−2.41	+1.58
Al I	2.34	2	0.03	−4.13	−0.16
Si I	4.05	2	-	−3.25	+0.72
K I	<0.89	2	-	<−4.06	<−0.09
S I	<5.09	1	-	<−2.12	<+1.78
Ca I	2.73	10	0.17	−3.63	+0.35
Sc II	−0.70	5	0.14	−3.87	+0.10
Ti I	1.40	8	0.09	−3.62	+0.35
Ti II	1.41	21	0.15	−3.61	+0.36
Cr I	1.29	5	0.10	−4.38	−0.41
Mn I	0.61	2	0.01	−4.78	−0.81
Co I	1.28	4	0.07	−3.64	+0.33
Ni I	2.19	3	0.02	−4.06	−0.07
Zn I	1.29	1	-	−3.41	+0.70
Sr II	−0.72	2	0.06	−3.64	+0.33
Y II	−1.80	3	0.11	−4.04	−0.07
Ba II	−2.42	4	0.10	−4.55	−0.58
Sm II	<−1.82	1	-	<−2.83	<+1.14
Eu II	<−3.42	1	-	<−3.93	<+0.04

Our analysis confirms the large overabundances of carbon and nitrogen in CS 22949–037 ([C/Fe] = +1.17±0.1, [N/Fe] = +2.56 ± 0.2, see Table 3 and Fig. 2), in good agreement with the results of Norris et al. (2001). But as an important new result, we have also been able to measure the $^{12}C/^{13}C$ ratio from ^{13}CH lines of both the $A^2\Delta - X^2\Pi$ and $B^2\Sigma - X^2\Pi$ systems. Using a total of 9 lines of ^{13}CH (6 from the $A^2\Delta - X^2\Pi$ system and 3 from the $B^2\Sigma - X^2\Pi$ system), we find $^{12}C/^{13}C = 4.0 \pm 2$ (Fig. 3). We note that the wavelengths for the ^{13}CH lines arising from the $A^2\Delta - X^2\Pi$ system were systematically ∼0.2 Å larger than observed, so the wavelengths for the whole set of lines was corrected by this amount.

Our derived $^{12}C/^{13}C$ ratio is much smaller than that found in metal-poor dwarfs: $^{12}C/^{13}C = 40$ (Gratton et al. 2000), and is close to the equilibrium isotope ratio reached in the CN cycle

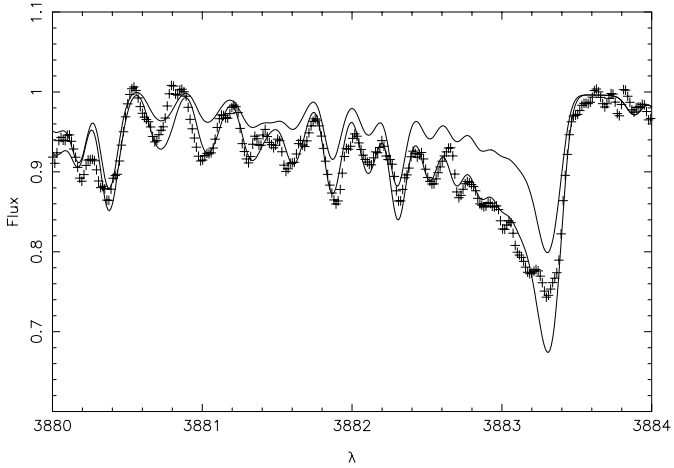

Fig. 2. Comparison of the observed spectrum (crosses) and synthetic spectra (thin lines) computed for [C/H] = −2.80, and [N/Fe] = 2.56 and +2.26., respectively.

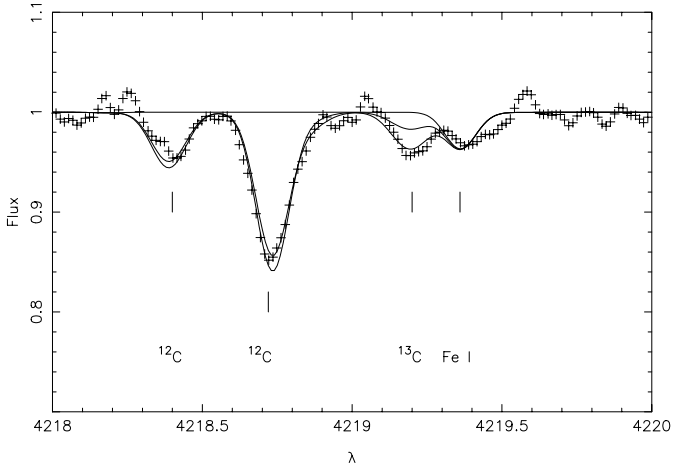

Fig. 3. Comparison of the observed spectrum (crosses) and synthetic profiles (thin lines) for $A^2\Delta - X^2\Pi$ ^{12}CH and ^{13}CH lines computed for $^{12}C/^{13}C$ = 4 and 10, and with no ^{13}C.

($^{12}C/^{13}C$ = 3.0). Note also that the observed $^{13}C/^{14}N$ ratio (assuming that the N abundance is solely ^{14}N) is about 0.03, close to the equilibirum value of 0.01 (Arnould et al. 1999). We conclude that the initial CNO abundances of CS 22949-037 have probably been modified by material processed in the equilibrium CN-cycle operating in the interior of the star, and later mixed into the envelope.

The very large nitrogen abundance of CS 22949–037 ([N/Fe] = +2.6) has been recently confirmed by Norris et al. (2002) from the NH band at 336–337 nm. Such large overabundances of nitrogen have previously been noted in two other carbon-enhanced metal-poor stars, CS 22947–028 and CS 22949–034 (Hill et al. 2000); ([N/Fe] = +1.8 and [N/Fe] = +2.3, respectively), but in these stars the carbon overabundance was much larger than in CS 22949–037 ([C/Fe] = +2.0 and [C/Fe] = +2.5, respectively). Norris et al. (1997a) also found a very nitrogen-rich star, CS 22957–027, with [N/Fe] = +2. Note, however, that Bonifacio et al. (1998) obtained [N/Fe] = +1 for this star, but this discrepancy can

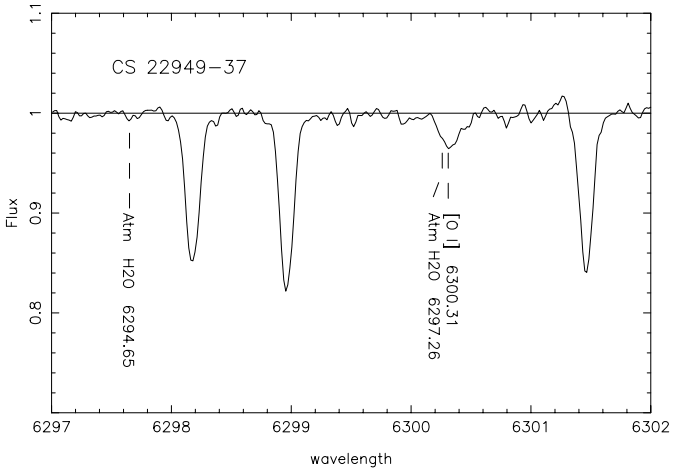

Fig. 4. Mean spectrum of CS 22949–037 from August 2000. The two telluric H_2O lines are indicated (shifted in wavelength by about 3 Å due to the radial velocity of the star).

be probably accounted for by differences in oscillator strenghs adopted for the CN band.

Oxygen

The most significant result of this study is that we have detected the forbidden [O I] line at 630.031 nm – the first time that the oxygen abundance has been measured in a star as metal deficient as CS 22949–037. The equivalent width of this feature, measured directly from the spectrum, is about 6 mÅ. The [O I] line occurs in a wavelength range plagued by telluric bands of O_2, but the radial velocity of CS 22949-037 shifts the oxygen line to a location that is far away from the strongest telluric lines in all our spectra. Moreover, the position of the [O I] line relative to the telluric lines is different in the spectra obtained in August 2000 and September 2001 (the heliocentric correction varies from 3 to 16 km s^{-1}), which provides valuable redundancy in our analysis.

In the August 2000 spectra a weak telluric H_2O line (λ = 629.726 nm) is superimposed on the stellar [O I] line (Fig. 4). We have accounted for this H_2O line in two different ways. First, we have estimated its intensity using that of another line from the same molecular band system (R1 113), a feature observed at 629.465 nm, which should be twice as strong as the line at 629.726 nm. Secondly, we have observed the spectrum of a blue star just before that of CS 22949–037, and at about the same airmass. Figure 5 shows the spectrum of the comparison star, and Fig. 6 the result of dividing our spectra of CS 22949–037 by it.

From the telluric line at 629.465 nm in the spectrum of CS 22949–037 (Fig. 4), we estimate the equivalent width of the line at 629.726 nm to be ∼1.5 mÅ. The equivalent width of the [O I] line itself should thus be about 4.5 ± 1.5 mÅ. From Fig. 6, the equivalent width of the O I line is 5 mÅ.

In our September 2001 spectrum of CS 22949–037 (Fig. 6) the telluric H_2O line falls outside the region of the stellar [O I] line, but the S/N ratio of that spectrum is much lower (Table 1). The measured equivalent width of the [O I] line from this

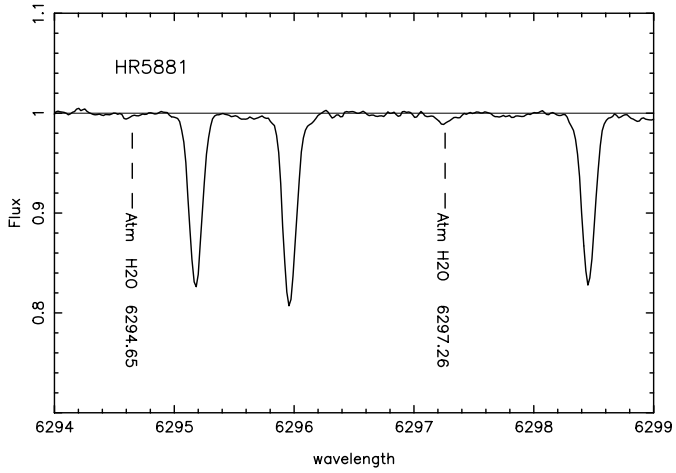

Fig. 5. Mean spectrum of the comparison star HR 5881 (A0 V, $v \sin i$ = 87 km s^{-1}), observed just before CS 22949–037.

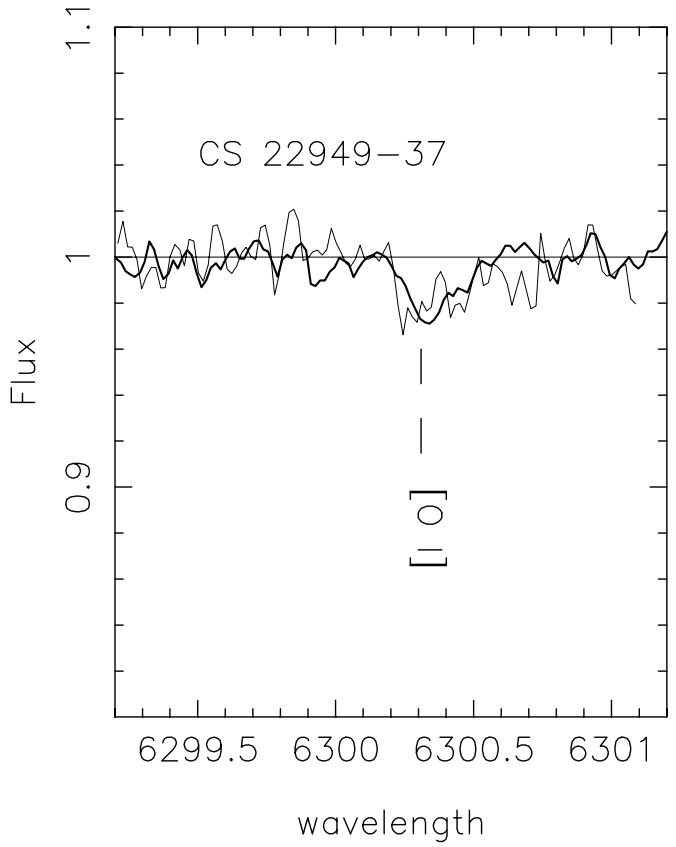

Fig. 6. The spectrum of CS 22949–037 divided by that of HR 5881 to eliminate the telluric lines (heavy line: mean of the three spectra obtained in August 2000 spectrum; thin line: September 2001 spectrum). The scale of both axes is the same as in Fig. 4. The measured equivalent width of the corrected [O I] line is 5 mÅ.

spectrum is 5 ± 2 mÅ, again in good agreement with the previous result. Our final value for the equivalent width of the [O I] line at 630.031 nm is then 5.0 ± 1.0 mÅ, corresponding to [O/H] = −1.98 ± 0.1 and [O/Fe] = +1.99 ± 0.1.

According to Kiselman (2001) and Lambert (2002), the [O I] feature is not significantly affected by non-LTE effects

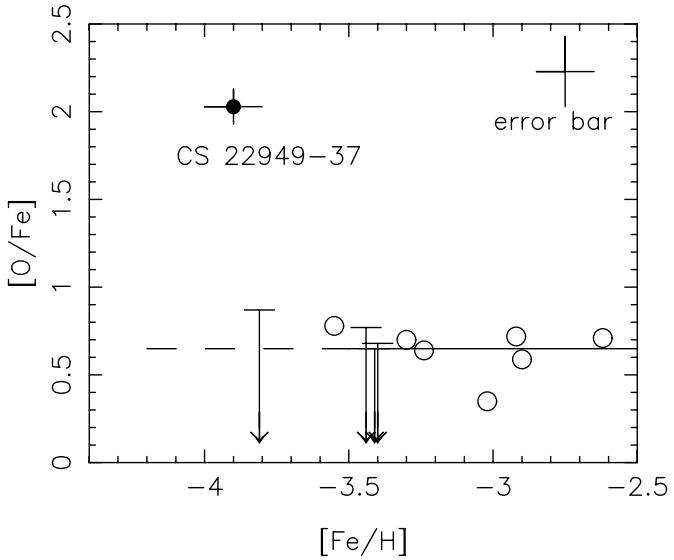

Fig. 7. Oxygen abundance from the [O I] forbidden line in extremely metal-poor stars: CS 22949–037 (black dot, this paper); measured values (open circles) and upper limits (arrows) in an extended sample (paper in preparation). At low metallicities, the ratio [O/Fe] does not seem to depend on [Fe/H], and is about +0.65. CS 22949–037 is thus very oxygen rich compared to "normal" extremely metal-poor stars. The error bar in the upper right corner is the typical uncertainty associated with the abundance determination in the sample. CS 22949–037 is plotted with its own associated uncertainties.

because (a) the line is weak, (b) the transition is a forbidden one (with collisional rates largely dominating over radiative rates), and (c) the upper level is collisionally excited. Oxygen abundances derived from the [O I] line are therefore less prone to systematic errors, but the line is very weak in metal-poor stars, hence high resolution and S/N ratio are both required.

Our result that [O/Fe] ≈ +2.0 in CS 22949–037, the most metal-poor star with a measured O abundance, raises the question whether such a large overabundance of O is representative of the most metal-poor stars in general. This would be an argument in favour of a continued increase of [O/Fe] at the lowest metallicities (e.g., Israelian et al. 2001a, 2001b).

Our VLT programme includes a sample of XMP giants which were observed and analysed in *exactly the same way* as CS 22949–037 (Depagne et al., in preparation). To provide a meaningful comparison to CS 22949–037, the oxygen abundances derived for this sample (from the [O I] line) are shown in Fig. 7. We stress once again that these abundance measurements have been obtained using exactly the same analysis as described in this paper, applied to 11 stars with effective temperatures between 4700 K and 4900 K, surface gravities between 0.8 to 1.8 dex, and metallicities in the range −2.6 to −3.8. The comparison between the oxygen abundance in CS 22949–037 and the rest of the sample is therefore straighforward, free from systematics arising from the method itself (e.g., determination of stellar parameters, atmospheric models, choice of oxygen indicator). In the metallicity range −3.5 ≤ [Fe/H] ≤ −2.5 we find a mean [O/Fe] ≈ +0.65, with surprisingly little scatter. We therefore expect that at [Fe/H] = −4.0,

the mean oxygen abundance should also be around [O/Fe] ≈ +0.65, as is also hinted at by the upper limit obtained on the [Fe/H] = −3.8 giant plotted in Fig. 7. (This point will be discussed in detail, and with a larger sample of stars, in a subsequent paper in this series). Note that CS 22949–037 is the only one of the giants in our program with [Fe/H] ≈ −4.0 in which we *could* detect the [O I] line: for [O/Fe] = +0.65 the predicted equivalent width is ≈0.2 mÅ, well below the normal detection threshold at this wavelength (0.5–1.0 mÅ, depending on the S/N of the spectra).

We thus conclude that the O abundance in CS 22949–037 is *not* typical for XMP stars; [O/Fe] appears to be ∼1.3 dex higher than the expected abundance ratio for stars of this low metallicity (Fig. 7).

We return to the discussion of the origin of these remarkable CNO abundances in Sect. 4.

3.2.2. The α elements Mg, Si, Ca, and Ti

In Fig. 8 we compare the light-element abundances of CS 22949–037 with those of the well-established XMP giants (the "classical" sample) studied by Norris et al. (2001).

The Si abundance in CS 22949–037 has been determined from two lines at 390.553 nm and 410.274 nm. The first is severely blended by a CH feature, while the latter falls in the wing of the H_δ line. These blends have been taken into account in the analysis, and both lines yield similar abundances. The 869.5 nm and 866.8 nm lines of sulphur are not detected, and yield a fairly mild upper limit of [S/Fe] ≤ +1.78.

The even-Z (α-) elements Mg, Si, Ca, and Ti are expected to be mainly produced during hydrostatic burning in stars, and are generally observed to be mildly enhanced in metal-poor halo stars. It is thus remarkable that, in CS 22949–037, the magnitude of the α-enhancement decreases with the atomic number of the element: [Mg/Fe] is far greater than normal, while the enhancement of the heaviest α-elements, like Ca and Ti, is practically the same as in the classical metal-poor sample (a point noted as well by Norris et al. 2001). The [Si/Fe] ratio has an intermediate value.

3.2.3. The light odd-Z elements Na, Al, and K

The abundances of the odd-Z elements Na, Al, and K in XMP stars are all derived from resonance lines that are sensitive to non-LTE effects. The Al abundance is based on the resonance doublet at 394.4 and 396.2 nm. Due to the high resolution and S/N of our spectra, both lines can be used, and the CH contribution to the Al I 394.4 nm line is easily taken into account. The Na I D lines are used for the Na abundance determination, while the K resonance doublet is not detected in CS 22949–037.

Derived [Na/Fe] and [Al/Fe] ratios are usually underabundant in XMP field stars (Fig. 8), while we find [K/Fe] to be generally overabundant in the classical XMP sample (Depagne et al., in preparation), in agreement with Takeda et al. (2002). As found already by McWilliam et al. (1995), Na is *strongly enhanced* in CS 22949–037 ([Na/Fe] = +2.08),

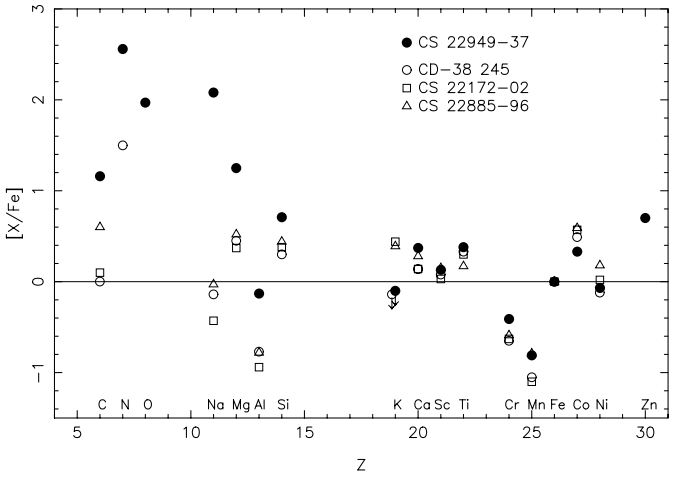

Fig. 8. Abundance of the elements from C to Zn in CS 22949–037 (filled circles) and in classical XMP stars with [Fe/H] ≈ −4 (open symbols). N, Mg, and Al are strongly enhanced in CS 22949–037, while the behaviour of the subsequent elements is normal.

while Al is less deficient than normal: [Al/Fe] = −0.13 in CS 22949–037, while the mean value for the comparison sample is [Al/Fe] = −0.8. The K doublet is undetected in both CS 22949–037 and CD –38 245, corresponding to upper limits of [K/Fe] ≤ −0.1 and [K/Fe] ≤ −0.14, respectively.

Several authors have pointed out that, in LTE analyses, the Na abundance may be overestimated (Baumüller et al. 1998), and the Al and K abundances underestimated (Baumüller & Gehren 1997; Ivanova & Shimanskii 2000; Norris et al. 2001). Following Baumüller et al. (1998) and Baumüller & Gehren (1997), for dwarfs with [Fe/H] = −3.0, LTE analysis leads to an offset of Δ[Al/H] ≈ −0.65 and Δ[Na/H] ≈ 0.6. Under the hypothesis of LTE, Al and Na behave similarly in dwarfs and giants, and as a first approximation we can therefore assume that the correction is the same for giants as for dwarfs (Norris et al. 2001).

However, the atmospheric parameters of all the stars shown in Fig. 8 are very similar ($4850 < T_{\rm eff} < 5050$ K, $1.7 < \log g < 2$, and [Fe/H] ≈ −4), so the NLTE effects must also be very similar for all four stars. Accordingly, the difference between the Na, Al, and K abundances in CS 22949–037 and in the classical metal-poor sample must be real and independent of the non-LTE effects. Figure 9 shows the differences between the light-element abundances in CS 22949–037 and the mean of the three XMP giants CD–38 245, CS 22172–02, and CS 22885–96. For potassium, the upper limit derived above for CD–38 245 was taken as the best approximation to the K abundance of this star when forming the mean. Figure 9 highlights the dramatic decrease in the enhancement of the light elements from Na through Si in CS 22949–037; beyond silicon, the abundance ratios in CS 22949–037 are similar to those in other XMP stars.

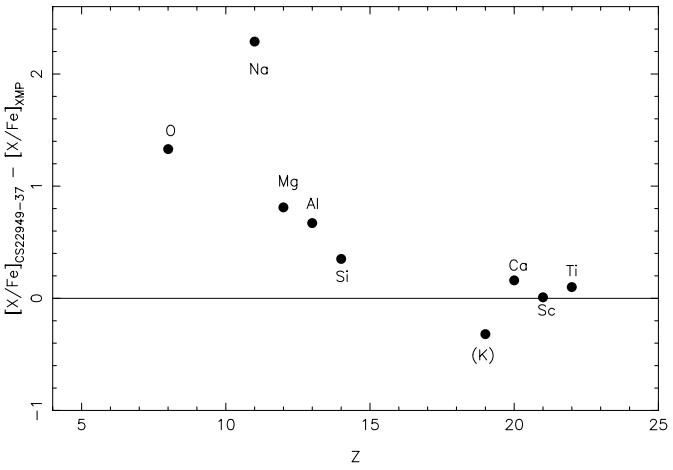

Fig. 9. $[X/Fe]_{22949-037} - [X/Fe]_{XMP}$, where "XMP" represents the mean abundances of the light elements of the three XMP giants CD –38°245, CS 22172–02, and CS 22885–96.

3.2.4. The Si-burning elements

The distribution of the abundances of the Si-burning elements in CS 22949–037 is different from that observed in the Sun, but is rather similar to the distribution observed in three other very metal-poor stars (see Fig. 8). Furthermore, this pattern is rather well represented by the Z35C zero-metal supernova yields obtained by Woosley & Weaver (1995), as modified by Woosley and Heger (model Z35Z, A. Heger, private communication). Note that Cr and Mn are underabundant while Co and Zn are overabundant. The present analysis of CS 22949-037 is the first case in which a Zn abundance has been derived in such an extremely metal-poor star. We find that [Zn/Fe] = +0.7 ± 0.1, in agreement with the increasing trend suggested in other very metal-poor stars (e.g., Primas et al. 2000; Blake et al. 2001), but of course it should be kept in mind that this star may not reflect the general behavior of the most metal-deficient stars.

3.2.5. The neutron-capture elements

CS 22949–037 is a carbon-rich XMP giant, and the neutron-capture elements are often (though not always) enhanced in such stars (e.g., Hill et al. 2000). Sr is indeed enhanced in CS 22949–037 ([Sr/Fe] = +0.33), but the [Y/Fe] ratio is about solar ([Y/Fe] = −0.07). Ba is underabundant relative to iron ([Ba/Fe] = −0.58) while Sm and Eu are not detected at all ([Eu/Fe] ≤ 0.04). In seeking an explanation for the origin of this pattern, we compare the distribution of heavy elements in CS 22949–037 to three well-studied groups of stars: (i) the classical XMP sample; (ii) the so-called CH stars, a well-known class of carbon-rich metal-poor stars, and (iii) the new class of mildly carbon-rich metal-poor stars without neutron-capture excess (Aoki et al. 2002). We have excluded the *r*-process enhanced XMP star CS 22892-052, as its mild carbon enhancement ([C/Fe] ≈ +1) appears to be unique among the presently known examples of this class.

(i) The classical XMP stars. In the three classical XMP giants (Norris et al. 2001), both Sr and Ba are very deficient with respect to iron, and by about the same factor: $[Sr/Fe]_{mean} = -1.16$, $[Ba/Fe]_{mean} = -1.15$ and $[Ba/Sr]_{mean} \approx 0.0$. In CS 22949–037, Sr is actually enhanced and [Ba/Sr] = −0.91, which is a rather different pattern.

(ii) The CH stars. As a group, the CH stars are moderately metal-poor ([Fe/H] = −1.5) yet strongly enriched in neutron-capture elements; most of them presumably formed as the result of the *s*-process inside an AGB star (Vanture 1992). The CH stars are members of long-period binary systems with orbital characteristics consistent with the presence of a fainter companion, and it is generally assumed that the abundance anomalies in these stars are the result of mass transfer from the AGB companion, which has now evolved into a white dwarf. At least one very metal-poor star is known to share many of these properties (LP 625-44; Norris et al. 1997a), and it too is a member of a binary system. More recently, Aoki et al. (2000) have confirmed the earlier work that suggested the level of [Sr/Ba] increases with atomic number (at contrast with our star), as expected from an *s*-process at high neutron exposure (e.g. Wallerstein et al. 1997; Gallino et al. 1998). For example, in some of these very metal-poor CH stars, ^{208}Pb is extremely overabundant (Van Eck et al. 2001); this element is not even detected in our star. In CS 22949–037 the situation is the opposite: the heavy-element abundances *decrease* with atomic number and even turn into a deficit ([Sr/Fe] = +0.33, [Y/Fe] = −0.07, and [Ba/Fe] = −0.58). Accordingly, the neutron-exposure processes in CS 22949–037 and the CH stars appear to have been completely different. Moreover, there is no indication that CS 22949–037 belongs to a binary system (cf. Table 1 and Sect. 2), but since the CH stars are generally long-period, low-amplitude binaries we cannot exclude that our star has been enriched by a companion. Accurate longer-term monitoring of the radial velocity of CS 22949–037 will be needed to settle this point.

(iii) The carbon-rich metal-poor stars without neutron-capture excess

Norris et al. (1997b), Bonifacio et al. (1998) and Aoki et al. (2002) observed five very metal-poor, carbon-rich giants (−3.4 < [Fe/H] < −2.7) without neutron-capture element excess. Like CS 22949–037, these stars exhibit carbon excesses of [C/Fe] ≈ +1, but $^{12}C/^{13}C \approx 10$. the nitrogen excesses in these stars is much smaller (0.0 < [N/Fe] < 1.2), and the neutron-capture abundances are about the same as in normal halo giants with [Fe/H] ≈ −3. Sr and Ba are underabundant, but the [Ba/Sr] ratio is close to solar, again completely unlike CS 22949–037. Aoki et al. (2002) have suggested that this class of stars could be the result of helium shell flashes near the base of the AGB in very low-metallicity, low-mass stars, but this hypothesis is not yet confirmed.

In summary, the detailed abundance patterns in CS 22949–037 appear to require a different origin from that of the currently known groups of carbon-rich XMP giants. This point is discussed further in the next section.

4. Comparison of the abundance pattern of CS 22949–037 with various theoretical studies

This early generation star is not the first one to display an abundance pattern that is not easily accounted for by standard SN II nucleosynthesis computations. The HK survey has found several very iron-poor stars with large abundances of C, and N (e.g., Hill et al. 2000). Figure 8 compares the abundances in CS 22949–037 with those of 3 classical metal-poor stars, which are passably explained by current SN II nucleosynthesis (Tsujimoto et al. 1995; Woosley & Weaver 1995), although no nitrogen (which is by-passed in a pure helium core) is predicted in our star and in CD–38°245, at contrast with the observations. Figure 9 gives the ratios of the abundances in CS 22949–037 to the mean of the 3 stars. Very clearly the major feature is a large relative overabundance with respect to iron of the light elements C, N, O, Na, and Mg, declining to almost insignificance at Si, and none for $Z > 15$, as already noted in Norris et al. (2001). Qualitalively, something very similar is occurring in the model Z35B of Woosley & Weaver (1995) which, because of insufficient explosion energy and partial "fallback", expels only C, O, Ne, Na, Mg, Al, a very small quantity of Si, and nothing heavier. Below we discuss several attempt to refine this idea.

Another path was followed by Norris et al. (2002) for explaining CS 22949–037: the pair-instability hypernova yields (see Fryer et al. 2001; and Heger & Woosley 2002). Here one important ingredient is the mixing of some of the carbon in the helium core with proton-rich material, producing a large amount of primary nitrogen. However, the other yields of pair-instability supernovae have some features which poorly fit the more complete pattern we have obtained here for CS 22949–037. In particular, they show a larger odd/even effect than the one seen in the star, and a small [Zn/Fe] , in contrast to the observed value of [Zn/Fe] = +0.7. So, it seems that, if the idea of primary nitrogen production by mixing must be retained, the case for pair-instability hypernovae is not attractive.

A large body of other theoretical work is relevant to the nucleosynthesis in very low-metallicity stars, and we make no attemps to fully sumarize previous results in the present papaer. However, a few recent ideas are worth keeping in mind. For example, Umeda & Nomoto (2002) have tried to explain the [Zn/Fe] $\approx$ 0.5 found at very low metallicity. Their conclusion is that the solution is a combination of a proper mass cut, followed by mixing between the initial mass cut and the top of the incomplete Si-burning region, followed by a fallback of most of the Si-burning region. In order to produce the usual [O/Fe] value and [Zn/Fe] $\approx$ 0.5, it is necessary to have a progenitor mass of 25 or 30 $M_{\odot}$, *and* an energetic explosion of 10 to 30×10^{51} ergs.

Chieffi & Limongi (2002) have explored the possibility of adjusting the free parameters in a single SN II event to fit the abundances of five individual very metal-poor stars (Norris et al. 2001, including CS 22949–037). Although in the end they discard CS 22949–037, they note that, except for the overabundance of C to Mg, the star is very similar to the other stars of the sample, and that the high [Co/Fe] value is apparently well explained in all C-rich stars by their computed yields.

Finally, we come back to the "fallback" explanation for the high, C,N,O, and Na abundances, which make this [Fe/H] = −4 star a $Z = 0.01\ Z_{\odot}$ star. An unpublished result (model Z35Z of Woosley & Heger, in preparation) was kindly communicated to us as a variant of the already cited model Z35C. This model has a slightly larger amount of fallback, and includes hydrodynamical mixing in the explosion. It shows a fairly good fit with our observations (crosses in Fig. 10), except for Al and Na, which have to be corrected for non-LTE effects, and for N, which is not expected to be formed in the Z35Z model. To improve this fit we corrected for the non-LTE effects on Na and Al (see Sect. 3.2.3), and we supposed (open circles in Fig. 10) that the observed abundance of nitrogen was the result of a transformation of carbon into nitrogen through the CN cycle (in the star itself or in its progenitor). After these corrections the agreement is much better. The discrepancy about the Zn abundance is probably curable (Umeda & Nomoto 2002) as explained here above.

At this point we must mention that rotation may be a source of mixing and CN processing (see Meynet & Maeder 2002), and that other non-standard mixing mechanisms have been investigated along the RGB, which may have altered the $^{12}C/^{13}C$ ratio and the C/N ratio in CS 22949–037 itself (Charbonnel 1995).

The computation of the supernova yields does not contain predictions for the neutron-capture elements. Generally speaking, these elements are not easily built in zero-metal supernovae (like Z35Z), nor in zero-metal very massive objects, owing to an inefficient neutron flux, a lack of neutron seeds or both. The main phenomenon observed in CS 22949–37 is the very rapid decline of the abundance of these elements with the atomic number. Such a decline is not observed in other very metal-poor stars (see Sect. 3.2.5), and it suggests an unusually "truncated" neutron exposure (very short relative to the neutron flux).

In summary, it appears that SNe II of mass near 30 $M_{\odot}$, either primordial or of very low metallicity, offer good prospects for explaining stars like CS 22949–037. Enough ingredients are available. They have still to be assembled in the most economic way.

5. Conclusions

Bringing the light collecting power, resolution, and extended wavelength coverage of UVES/VLT to bear on the abundance analysis of CS 22949–37 has provided important new results as well as refined the results of previous analyses. For the first time in such a metal-poor star, we have measured the forbidden O I line at 630.0 nm: we found [O/Fe] = +1.97. We found a mild carbon enhancement [C/Fe] = +1.17 and a very low $^{12}C/^{13}C = 4 \pm 2$ ratio, close to the equilibrium value The elemental abundances of the extremely metal-poor stars CS 22949–037 are very unusual. The strong enhancement of oxygen (not typical for this very low metallicity) could be explained by pair-instability supernovae, but the strong odd-even effect predicted in these models, which is not observed, rules out these very massive objects. The enhancement of O and C is explained by models of zero-metallicity (or very metal-poor)

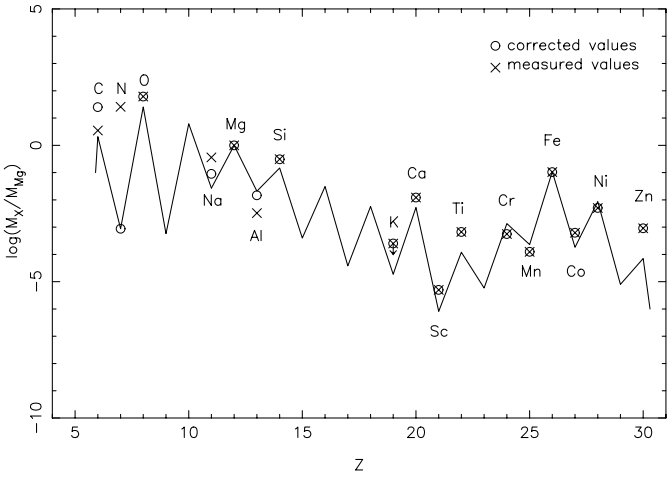

Fig. 10. The logarithmic mass ratio of elements X to Mg (log M_X/M_{Mg}) compared with those predicted by the zero heavy-element supernova model Z35Z (Woosley & Weaver 1995, as recently modified by Heger and Woosley). The measured abundances in CS 22949–037 have been corrected for NLTE effects (Na, Al), or for internal mixing in the star (C, N). The open circles represent the assumed initial abundances of the elements, while the crosses show the atmospheric abundances as derived in LTE. For K, only an upper limit is available.

core-collapse supernovae. The observed enhancement of N has to be explained by the CN processing of C, in the supernova or in the star itself (or its companion, if binary). The fair agreement between the observed elemental abundances in CS 22949–037 and those predicted in the Z35Z model of Woosley and Heger (private communication) suggests that the most likely interpretation is that this star exhibits the ejecta of a single core-collapse supernova. However, more complex scenarios, in which the combined ejecta of several progenitors are responsible, are not excluded by the present data. Clearly, interpretation of the exceptional pattern of the neutron-capture elements in CS 22949–037 merits further study. The identification of other extremely metal-poor stars that exhibit similar patterns would be most illuminating.

Acknowledgements. We thank A. Heger, S. Woosley, I. Baraffe, A. Chieffi and L. Limongi for useful discussions pertaining to the interpretation of the elemental abundance patterns in CS 22949-037, in particular A. Heger and S. Woosley for kindly providing the modified supernova yields and A. Chieffi and L. Limongi for sending us a copy of their paper in advance of publication their paper. We thank N. Jacquinet-Husson for helping to extract accurate wavelengths of the telluric lines from the GEISA database. We also thank the referee, J. Cowan, for useful comments that helped to improve the paper. J.A. and B.N. received partial support for this work from the Carlsberg foundation and the Danish Natural Science Research Council. T.B. acknowledges partial support of this work from the U.S. National Science Foundation, in the form of grants AST 00-98549 and AST 00-98508.

Appendix A: Line list and atomic data

We list in this table all the lines that were used to derive abundance.

Table .1. Linelist, equivalent width, and abundance for the elements in CS 22949–937.

Element					< log ϵ >
	lambda	log (gf)	W (mÅ)	log ϵ	
O1					**6.84**
	6300.304	−9.750	5.0	6.84	
Na1					**3.80**
	5889.951	0.110	151.6	3.82	
	5895.924	−0.190	132.9	3.77	
Mg1					**5.17**
	3829.355	−0.210	156.1	5.19	
	3832.304	0.150	185.2	5.12	
	3838.290	0.420	202.7	4.85	
	4167.271	−1.000	46.3	5.54	
	4571.096	−5.390	52.9	5.07	
	5172.684	−0.380	176.1	5.22	
	5183.604	−0.160	199.4	5.23	
	5528.405	−0.340	62.6	5.08	
Al1					**2.34**
	3944.006	−0.640	71.5	2.36	
	3961.520	−0.340	84.1	2.32	
Si1					**4.05**
	4102.936	−2.700	16.4	4.26	
Ca1					**2.73**
	4226.728	0.240	112.5	2.67	
	4283.011	−0.220	15.4	3.12	
	4318.652	−0.210	6.1	2.67	
	4454.779	0.260	19.4	2.77	
	5588.749	0.210	4.1	2.70	
	5857.451	0.230	1.0	2.51	
	6102.723	−0.790	2.3	2.70	
	6122.217	−0.320	8.1	2.81	
	6162.173	−0.090	11.4	2.76	
	6439.075	0.470	5.1	2.52	
Sc2					**−0.70**
	4246.822	0.240	62.7	−0.72	
	4314.083	−0.100	37.8	−0.47	
	4400.389	−0.540	11.7	−0.71	
	4415.557	−0.670	8.5	−0.75	
	5031.021	−0.400	2.0	−0.84	
Ti1					**1.40**
	3998.636	−0.060	11.9	1.35	
	4533.241	0.480	7.2	1.44	
	4534.776	0.280	3.4	1.29	
	4981.731	0.500	9.0	1.48	
	4991.065	0.380	6.5	1.45	
	4999.503	0.250	5.8	1.51	
	5173.743	−1.120	1.8	1.38	
	5192.969	−1.010	1.7	1.27	
Ti2					**1.41**
	3759.296	−0.460	117.7	2.24	
	3761.323	0.100	114.6	1.56	
	3913.468	−0.530	67.0	1.54	
	4012.385	−1.610	31.9	1.28	
	4028.343	−1.000	5.4	1.28	
	4290.219	−1.120	37.4	1.55	
	4337.915	−1.130	35.1	1.42	

Table .1. continued.

Element					< log ϵ >
	lambda	log (gf)	W (mÅ)	log ϵ	
	4395.033	−0.660	56.9	1.34	
	4395.850	−2.170	2.8	1.37	
	4399.772	−1.270	22.1	1.46	
	4417.719	−1.430	24.5	1.59	
	4443.794	−0.710	51.5	1.29	
	4450.482	−1.450	19.1	1.37	
	5226.543	−1.290	6.10	1.165	
Cr1					**1.29**
	4254.332	−0.110	38.2	1.16	
	4274.796	−0.230	35.7	1.23	
	4289.716	−0.360	31.8	1.28	
	5206.038	0.020	10.9	1.33	
	5208.419	0.160	17.5	1.43	
Mn1					**0.61**
	4030.753	−0.480	26.6	0.60	
	4033.062	−0.620	21.2	0.61	
Fe1					**3.51**
	3899.700	−1.530	102.2	3.84	
	3920.300	−1.750	95.5	3.87	
	3922.900	−1.650	102.5	3.91	
	4005.200	−0.610	61.5	3.45	
	4045.800	0.280	99.6	3.46	
	4063.600	0.070	89.8	3.47	
	4071.700	−0.020	84.1	3.46	
	4076.600	−0.370	6.3	3.62	
	4132.100	−0.670	58.2	3.47	
	4143.900	−0.460	66.2	3.37	
	4147.700	−2.100	7.7	3.48	
	4156.800	−0.610	5.0	3.32	
	4174.900	−2.970	7.4	3.67	
	4181.800	−0.180	10.5	3.24	
	4187.000	−0.550	18.6	3.47	
	4187.800	−0.550	22.1	3.53	
	4191.400	−0.730	13.5	3.51	
	4195.300	−0.410	11.1	4.06	
	4199.100	0.250	23.9	3.49	
	4202.000	−0.700	60.3	3.38	
	4222.200	−0.970	8.3	3.48	
	4227.400	0.230	15.1	3.57	
	4233.600	−0.600	19.0	3.56	
	4250.100	−0.400	22.6	3.45	
	4260.500	−0.020	44.2	3.44	
	4271.200	−0.350	32.7	3.60	
	4271.800	−0.160	88.1	3.50	
	4282.400	−0.820	16.0	3.33	
	4325.800	−0.010	91.2	3.57	
	4404.800	−0.140	85.1	3.46	
	4415.100	−0.610	61.8	3.44	
	4447.700	−1.340	6.0	3.42	
	4461.700	−3.200	33.0	3.71	
	4466.600	−0.600	6.0	3.37	
	4494.600	−1.140	11.7	3.51	
	4528.600	−0.820	21.3	3.48	
	4871.300	−0.360	10.7	3.43	
	4872.100	−0.570	7.8	3.50	
	4891.500	−0.110	19.8	3.47	
	4919.000	−0.340	11.0	3.42	
	4920.500	0.070	23.5	3.36	
	4994.100	−3.080	7.5	3.72	
	5001.900	0.010	3.1	3.61	
	5041.100	−3.090	4.2	3.51	
	5041.800	−2.200	8.2	3.54	
	4494.600	−1.140	11.7	3.51	
	4528.600	−0.820	21.3	3.48	
	4871.300	−0.360	10.7	3.43	
	4872.100	−0.570	7.8	3.50	
	4891.500	−0.110	19.8	3.47	

Table .1. continued.

Element					< log ϵ >
	lambda	log (gf)	W (mÅ)	log ϵ	
	4919.000	−0.340	11.0	3.42	
	4920.500	0.070	23.5	3.36	
	4994.100	−3.080	7.5	3.72	
	5001.900	0.010	3.1	3.61	
	5041.100	−3.090	4.2	3.51	
	5041.800	−2.200	8.2	3.54	
	5049.800	−1.360	5.5	3.43	
	5051.600	−2.800	11.2	3.63	
	5068.800	−1.040	3.9	3.70	
	5110.400	−3.760	15.9	3.68	
	5123.700	−3.070	4.8	3.60	
	5127.400	−3.310	3.0	3.52	
	5166.300	−4.200	7.8	3.77	
	5171.600	−1.790	19.5	3.56	
	5194.900	−2.090	6.9	3.42	
	5232.900	−0.060	15.6	3.37	
	5266.600	−0.390	6.2	3.32	
	5324.200	−0.240	7.2	3.48	
	5328.500	−1.850	15.0	3.55	
	5339.900	−0.720	3.2	3.65	
	5371.500	−1.650	62.6	3.63	
	5383.400	0.640	2.3	3.32	
	5397.100	−1.990	46.8	3.64	
	5405.800	−1.840	44.8	3.53	
	5429.700	−1.880	48.5	3.60	
	5434.500	−2.120	31.5	3.59	
	5446.900	−1.910	43.8	3.58	
	5455.600	−2.090	33.4	3.59	
	5506.800	−2.800	9.4	3.59	
Fe2					**3.56**
	4178.862	−2.480	5.0	3.39	
	4233.172	−2.000	20.2	3.59	
	4416.830	−2.600	4.9	3.71	
	4515.339	−2.480	3.4	3.49	
	4520.224	−2.610	2.8	3.50	
	4555.893	−2.280	7.3	3.62	
Co1					**1.28**
	3845.461	0.010	30.9	1.35	
	3995.302	−0.220	16.7	1.20	
	4118.767	−0.490	7.9	1.24	
	4121.311	−0.320	17.2	1.30	
Ni1					**2.19**
	3807.138	−1.180	50.4	2.21	
	3858.292	−0.970	58.9	2.17	
	5476.900	−0.890	6.2	2.17	
	5476.900	−0.890	6.2	2.17	
Zn1					**1.29**
	4822.528	−0.13	3.0	1.29	
Sr2					**−0.72**
	4077.709	0.170	109.3	−0.67	
	4215.519	−0.170	95.5	−0.75	
Y2					**−1.80**
	3950.352	−0.490	7.7	−1.68	
	3950.352	−0.490	7.7	−1.68	
	4883.684	0.070	1.6	−1.90	
	5087.416	−0.170	1.2	−1.80	
Ba2					**−2.42**
	4554.029	0.170	23.1	−2.53	
	4934.076	−0.150	15.7	−2.46	
	5853.668	−1.010	0.7	−2.38	
	6141.713	−0.070	5.6	−2.30	
Sm2					**−1.82**
	4537.941	−0.230	1.3	−1.82	
Eu2					**−3.42**
	4129.725	0.200	1.00	−3.41	

References

Alonso, A., Arribas, S., & Martinez-Roger, C. 1999, A&AS, 140, 261
Alvarez, R., & Plez, B. 1998, A&A, 330, 1109
Aoki, W., Norris, J. E., Ryan, S. G., et al. 2000, ApJ, 536, 97
Aoki, W., Ryan, S. G., Norris, J. E., et al. 2001, ApJ, 561, 346
Aoki, W., Norris, J. E., Ryan, S. G., et al. 2002, ApJ, 567, 1166
Arnould, M., Goriely, S., & Jorissen, A. 1999, A&A, 347, 572
Asplund, M., Gustafsson, B., Kiselman, D., et al. 1997, A&A, 318, 521
Baumüller, D., & Gehren, T. 1997, A&A, 325, 1088
Baumüller, D., Butler, K., & Gehren, T. 1998, A&A, 338, 637
Bauschlicher, C. W., Langhoff, S. R., & Taylor, P. R. 1988, ApJ, 332, 531
Beers, T. C., Preston, G. W., & Shectman, S. A. 1992, AJ, 103, 1987
Beers, T. C., Rossi, S., Norris, et al. 1999, ApJ, 117, 981
Bessell, M., & Brett, J. M. 1988, PASP, 100, 1134
Blake, L., Ryan, S., Norris, J., et al. 2001, Nucl. Phys. A., 688, 502
Bonifacio, P., Molaro, P., Beers, T. C., et al. 1998, A&A, 332, 680
Burstein, D., & Heiles, C. 1982, AJ, 87, 1165
Cayrel, R. 1988, in The impact of Very High S/N Spectroscopy on Stellar Physics, ed. G. Cayrel de Strobel, & M. Spite (Kluwer Dordrecht), Proc. IAU Symp., 132, 345
Cayrel, R., Hill, V., Beers, T. C., et al. 2001, Nature, 409, 691
Cerny, D., Bacis, R., Guelachviliet, et al. 1978, JMS, 73, 154
Charbonnel, C. 1995, ApJ, 453, 41
Chieffi, A., Dominguez, I., Limongi, M., et al. 2001, ApJ, 554, 1159
Chieffi, A., & Limongi, M. 2002, ApJ, submitted
Cowan, J. J., Pfeiffer, B., Kratz, K. L., et al. 1999, ApJ, 521, 194
Dekker, H., D'Odorico, S., Kaufer, A., et al. 2000, in Optical and IR Telescope Instrumentation and Detectors, ed. I. Masanori, & F. A. Moorwood, Proc. SPIE, 4008, 534
Edvardsson, B., Andersen, J., Gustafsson, B., et al. 1993, A&A, 275, 101
Fryer, C. L., Woosley, S. E., & Heger, A. 2001, ApJ, 550, 372
Gallino, R., Arlandini, C., Busso, M., et al. 1998, ApJ, 497, 388
Gratton, R. G., Sneden, C., Carretta, E., et al. 2000, A&A, 354, 169
Gustafsson, B., Bell, R. A., Eriksson, K., et al. 1975, A&A, 42, 407
Heger, A., Woosley, S. E., Baraffe, I., et al. 2002 [astro-ph/0112059]
Heger, A., & Woosley, S. E. 2002, ApJ, 567, 532
Hill, V., Plez, B., Cayrel, R., et al. 2002, A&A, submitted
Hill, V., Barbuy, B., Spite, M., et al. 2000, A&A, 353, 557
Ito, H., Ozaki, Y., Suzuki, K., et al. 1988, JMS, 127, 283
Israelian, G., Rebolo, R., García López, R. J., et al. 2001a, ApJ, 557, L43
Israelian, G., Rebolo, R., García López, R. J., et al. 2001b, ApJ, 551, 833
Ivanova, D. V., & Shimansky, V. V. 2000, AZh, 77, 432 (English transl. in Astron. Rep., 44, 376)
Jørgensen, U. G., Larsson, M., Iwamae, et al. 1996, A&A, 315, 204
Kiselman, D. 2001, New Ast. Rev., 45, 559
Kotlar, A. J., Field, R. W., & Steinfeld, J. I. 1980, JMS, 80, 86
Lambert, D. L. 2002, in Highlights of Astronomy, 12, ASP, ed. H. Rickman, in press
Larsson, M., Siegbahn, P. E. M., & Agren, H. 1983, ApJ, 272, 369L
Luque, J., & Crosley, D. R. 1999, SRI International Report MP 99-009
Meynet, G., & Maeder, A. 2002, A&A, 381, L25
McWilliam, A., Preston, G. W., Sneden, C., et al. 1995, AJ, 109, 2757
Norris, J. E., Ryan, S. G., & Beers, T. C. 1996, ApJ, 471, 254
Norris, J. E., Ryan, S. G., & Beers, T. C. 1997, ApJ, 488, 350
Norris, J. E., Ryan, S. G., & Beers, T. C. 1997, ApJ, 489, L169
Norris, J. E., Ryan, S. G., & Beers, T. C. 2001, ApJ, 561, 1034
Norris, J. E., Ryan, S. G., Beers, T. C., et al. 2002, ApJ, 569, 107
Plez, B. 1998, A&A, 337, 495
Plez, B., Brett, J. M., & Nordlund, Å. 1992, A&A, 256, 551
Prasad, C. V. V., & Bernath, P. F. 1992, JMS, 156, 327
Prasad, C. V. V., Bernath, P. F., Frum, C., et al. 1992, JMS, 151, 459
Primas, F., Brugamyer, E., Sneden, C., et al. 2000, in The First Stars, ed. A. Weiss, T. Abel, & V. Hill (Springer Berlin), 51
Rehfuss, B. D., Suh, M. H., & Miller, T. A. 1992, JMS, 151, 437
Spite, F., & Spite, M. 1982, A&A, 115, 357
Takeda, Y., Zhao, G., Chen, Y.-Q., et al. 2002 [astro-ph/0110165]
Thornton, K., Gaudlitz, M., Janka, H.-T., et al. 1998, ApJ, 500, 98
Timmes, F. X., Woosley, S. E., & Weaver, T. A. 1995, ApJS, 98, 617
Umeda, H., & Nomoto, K. 2002 ApJ, 565, 385
Van Eck, S., Goriely, S., Jorissen, A., et al. 2001, Nature, 412, 793
Vanture, A. D. 1992, AJ, 104, 1986
Wallerstein, G., Iben, I., Parker, P., et al. 1997, Rev Mod. Phys., 69, in Synthesis of elements in stars: forty years of progress, Chapter XI, 1042
Woosley, S. E., & Weaver, T. A. 1995, ApJS, 101, 181